

MSRL: Distributed Reinforcement Learning with Dataflow Fragments

Huanzhou Zhu*
Imperial College London

Bo Zhao*
Imperial College London

Gang Chen
Huawei Technologies Co., Ltd.

Weifeng Chen
Huawei Technologies Co., Ltd.

Yijie Chen
Huawei Technologies Co., Ltd.

Liang Shi
Huawei Technologies Co., Ltd.

Yaodong Yang
Huawei R&D United Kingdom

Peter Pietzuch
Imperial College London

Lei Chen
Hong Kong University of Science and Technology

Abstract

Reinforcement learning (RL) trains many agents, which is resource-intensive and must scale to large GPU clusters. Different RL training algorithms offer different opportunities for distributing and parallelising the computation. Yet, current distributed RL systems tie the definition of RL algorithms to their distributed execution: they hard-code particular distribution strategies and only accelerate specific parts of the computation (e.g. policy network updates) on GPU workers. Fundamentally, current systems lack abstractions that decouple RL algorithms from their execution.

We describe *MindSpore Reinforcement Learning* (MSRL), a distributed RL training system that supports *distribution policies* that govern how RL training computation is parallelised and distributed on cluster resources, without requiring changes to the algorithm implementation. MSRL introduces the new abstraction of a *fragmented dataflow graph*, which maps Python functions from an RL algorithm’s training loop to parallel computational *fragments*. Fragments are executed on different devices by translating them to low-level dataflow representations, e.g. computational graphs as supported by deep learning engines, CUDA implementations or multi-threaded CPU processes. We show that MSRL subsumes the distribution strategies of existing systems, while scaling RL training to 64 GPUs.

1 Introduction

Reinforcement learning (RL) solves decision-making problems in which agents continuously learn policies, typically represented as deep neural networks (DNNs), on how to act in an unknown environment [48]. RL has achieved remarkable outcomes in complex real-world settings: in game play, AlphaGo [46] has defeated a world champion in the board game Go; in biology, AlphaFold [20] has predicted three-dimensional structures for protein folding; in robotics, RL-based approaches have allowed robots to perform tasks such as dexterous manipulation without human intervention [14].

The advances in RL come with increasing computational demands for training: AlphaStar trained 12 agents using 384 TPUs and 1,800 CPUs for more than 44 days to achieve grandmaster level in StarCraft II game play [50]; OpenAI Five trained to play Dota 2 games for 10 months with 1,536 GPUs and 172,800 CPUs, defeating 99.4% of human players [3]. Distributed RL systems must therefore scale in terms of agent numbers, the amount of training data generated by environments, and the complexity of the trained policies [3, 20, 50].

Existing designs for distributed RL systems, e.g. SEED RL [9], ACME [17], Ray [33], RLlib [24] and Podracer [15] hardcode a single strategy to parallelise and distribute an RL training algorithm based on its algorithmic structure. For example, if an RL algorithm is defined as a set of Python functions for agents, learners and environments, a system may directly invoke the implementation of an agent’s `act()` function to generate new actions for the environment.

While integrating an RL algorithm’s definition with its execution strategy simplifies the design and implementation, it means that systems fail to parallelise and distribute RL algorithms in the most effective way:

(1) When *parallelising* the training computation, most RL systems only accelerate the DNN computation on GPUs or TPUs [9, 17, 24] using current deep learning (DL) engines, such as PyTorch [38], TensorFlow [13] or MindSpore [18]. Other parts of the RL algorithm, such as action generation, environment execution and trajectory sampling, are left to be executed as sequential Python functions on worker nodes, potentially becoming performance bottlenecks.

Recently, researchers have investigated this unrealised acceleration potential: Podracer [15] uses the JAX [11] compilation framework to vectorise the Python implementation of RL algorithms and parallelise execution on GPUs and TPUs; WarpDrive [22] can execute the entire RL training loop on a GPU when implemented in CUDA; and RLlib Flow [25] uses parallel dataflow operators [54] to express RL training. While these approaches accelerate a larger portion of RL algorithms, they force users to define algorithms through custom APIs e.g. with a fixed set of supported computational operators.

*Equal contribution

(2) For the *distribution* of the training computation, current RL systems are designed with particular strategies in mind, i.e. they allocate algorithmic components (e.g. actors and learners) to workers in a fixed way. For example, SEED RL [9] assumes that learners perform both policy inference and training on TPU cores, while actors execute on CPUs; ACME [17] only distributes actors and maintains a single learner; and TLeague [47] distributes learners but co-locates environments with actors on CPU workers. Different RL algorithms deployed in different resources will exhibit different computational bottlenecks, which means that a single strategy for distribution cannot be optimal.

We observe that the above challenges originate from the lack of an *abstraction* that separates the *specification* of an RL algorithm from its *execution*. Inspired by how compilation-based DL engines use intermediate representations (IRs) to express computation [7, 52], we want to design a new distributed RL system that (i) supports the execution of arbitrary parts of the RL computation on parallel devices, such as GPUs and CPUs (*parallelism*); and (ii) offers flexibility how to deploy parts of an RL algorithm across devices (*distribution*).

We describe *MindSpore Reinforcement Learning* (MSRL), a distributed RL system that decouples the specification of RL algorithms from their execution. This enables MSRL to change how it parallelises and distributes different RL algorithms to reduce iteration time and increase the scalability of training. To achieve this, MSRL’s design makes the following contributions:

(1) Execution-independent algorithm specification (§3).

In MSRL, users specify an RL algorithm by implementing its *algorithmic components* (e.g. agents, actors, learners) as Python functions in a traditional way. This implementation makes no assumptions about how the algorithm will be executed: all runtime interactions between components are managed by calls to MSRL APIs. A separate *deployment configuration* defines the devices available for execution.

(2) Fragmented dataflow graph abstraction (§4).

From the RL algorithm implementation, MSRL constructs a *fragmented dataflow graph* (FDG). An FDG is a dataflow representation of the computation that allows MSRL to map the algorithm to heterogeneous devices (CPUs and GPUs) at deployment time. The graph consists of *fragments*, which are parts of the RL algorithm that can be parallelised and distributed across devices.

MSRL uses static analysis on the algorithm implementation to group its functions into fragments, instances of which can be deployed on devices. The boundaries between fragments are decided with the help of user-provided *partition annotations* in the algorithm implementation. Annotations specify synchronisation points that require communication between fragments that are replicated across devices for increased data-parallelism.

(3) Fragment execution using DL engines (§5).

For execution, MSRL deploys hardware-specific implementations of fragments, permitting instances to run on CPUs and/or GPUs. MSRL supports different fragment implementations: CPU implementations use regular Python code, and GPU implementations are generated as compiled computation graphs of DL engines (e.g. MindSpore or TensorFlow) if a fragment is implemented using operators, or they are implemented directly in CUDA. MSRL fuses multiple data-parallel fragments for more efficient execution.

(4) Distribution policies (§6).

Since the algorithm implementation is separated from execution through the FDG, MSRL can apply different *distribution policies* to govern how fragments are mapped to devices. MSRL supports a flexible set of distribution policies, which subsume the hard-coded distribution strategies of current RL systems: e.g. a distribution policy can distribute multiple actors to scale the interaction with the environment (like Acme [17]); distribute actors but move policy inference to learners (like SEED RL [9]); distribute both actors and learners (like Sebulba [15]); and represent the full RL training loop on a GPU (like WarpDrive [22] and Anakin [15]). As the algorithm configuration, its hyperparameters or hardware resources change, MSRL can switch between distribution policy to maintain high training efficiency without requiring changes to the RL algorithm implementation.

We evaluate MSRL experimentally and show that, by switching between distribution policies, MSRL improves the training time of the PPO RL algorithm by up to $2.4\times$ as hyperparameters, network properties or hardware resources change. Its FDG abstraction offers more flexible execution without compromising training performance: MSRL scales to 64 GPUs and outperforms the Ray distributed RL system [33] by up to $3\times$.

2 Distributed Reinforcement Learning

Next we give background on reinforcement learning (§2.1), discuss the requirements for distributed RL training (§2.2), and survey the design space of existing RL systems (§2.3).

2.1 Reinforcement learning

Reinforcement learning (RL) solves a sequential decision-making problem in which an *agent* operates in an unknown *environment*. The agent’s goal is to learn a *policy* that maximises the cumulative *reward* based on the feedback from the environment (see Fig. 1): **1** *policy inference*: an agent performs an inference computation on a policy, which maps the environment’s state to an agent’s action; **2** *environment execution*: the environment executes the actions, generating *trajectories*, which are sequences of $\langle \text{state}, \text{reward} \rangle$ pairs produced by the policy; **3** *policy training*: finally, the agent improves the policy by training it based on the received reward.

RL algorithms that train a policy fall into three categories: (1) *value-based* methods (e.g. DQN [32]) use a deep neural network (DNN) to approximate the value function, i.e. a map-

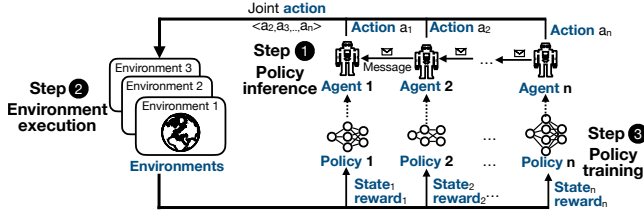


Fig. 1: RL training loop with multiple agents

ping of the expected return to perform a given action in a state. Agents learn the values of actions and select actions based on these estimated values; (2) *policy-based* methods (e.g. Reinforce [51]) directly learn a parametrised policy, approximated by a DNN, for selecting actions without consulting a value function. Agents use batched trajectories to train the policy by updating the parameters in the direction of the gradient that maximises the reward; and (3) *actor-critic* methods (e.g. PPO [45], DDPG [26], A2C [31]) combine the two by learning a policy to select actions (*actor*) and a value function to evaluate selected actions (*critic*).

Multi-agent reinforcement learning (MARL) has multiple agents, each optimising its own cumulative reward when interacting with the environment or other agents (see Fig. 1). A3C [31] executes agents asynchronously on separate environment instances; MAPPO [53] extends PPO to a multi-agent setting in which agents share a global parametrised policy. During training, each agent maintains a central critic that takes joint information (e.g. state/action pairs) as input, while learning a policy that only depends on local state.

2.2 Requirements for distributed RL systems

The benefits of RL come at the expense of its computational cost [37]. Complex settings and environments require the exploration of large spaces of actions, states and DNN parameters, and these spaces grow exponentially with the number of agents [35]. Therefore, RL systems must be scalable by exploiting both the parallelism of GPU acceleration and a large number of distributed worker nodes.

There exists a range of proposals how RL systems can parallelise and distribute RL training: for single-agent RL, environment execution (2 in Fig. 1), policy inference and training (1+3) can be distributed across workers [15, 17, 33], potentially using GPUs [9, 15]; for MARL, agents can be distributed [24, 25, 33, 43] and exchange training state using communication libraries [28, 36]. In general, environment instances can execute in parallel [15, 31] or be distributed [8] to speed up execution.

Not a single of the above strategies for parallelising and distributing RL training is optimal, both in terms of achieving the lowest iteration time and having the best scalability, for all possible RL algorithms. For different algorithms, training workloads and hardware resources, the training bottlenecks shift: e.g. our measurements show that, for PPO, environment execution (2) takes up to 98% of execution time; for MuZero [44], a large MARL algorithm with many agents,

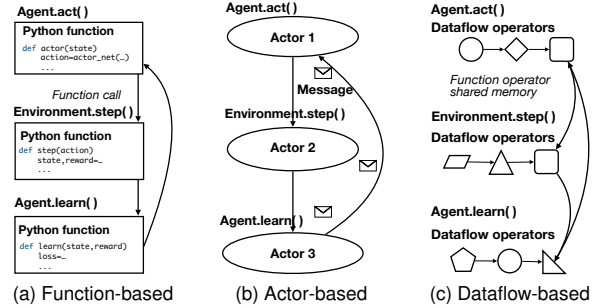


Fig. 2: Types of RL system designs

environment execution is no longer the bottleneck, and 97% of time is spent on policy inference and training (1+3).

Instead of hardcoding a particular approach for parallelising and distributing RL computation, a distributed RL system design should provide the flexibility to change its execution approach based on the workload. This leads us to the following requirements that our design aims to satisfy:

(1) **Execution abstraction.** The RL system should have a flexible execution abstraction that enables it to parallelise and distribute computation unencumbered by how the algorithm is defined. While such execution abstractions are commonplace in compilation-based DL engines [4, 7, 11, 42], they do not exist in current RL systems (see §2.3).

(2) **Distribution strategies.** The RL system should support different strategies for distributing RL computation across worker nodes. Users should be permitted to specify multiple distribution strategies for a single RL algorithm, switching between them based on the training workload, without having to change the algorithm implementation. Distribution strategies should be applicable across classes of RL algorithms.

(3) **Acceleration support.** The RL system should exploit the parallelism of devices, such as multi-core CPUs, GPUs or other AI accelerators. It should support the full spectrum from fine-grained vectorised execution to course-grained task parallel tasks on CPUs cores. Acceleration should not be restricted to policy training and inference only (1+3) but cover the full training loop, including environment execution (2) [22].

(4) **Algorithm abstraction.** Despite decoupling execution from algorithm specification, users expect familiar APIs for defining algorithms around algorithmic components [10, 12, 21], such as agents, actors, learners, policies, environments etc. An RL system should therefore provide standard APIs, e.g. defining the main training loop in terms of policy inference (1), environment execution (2) and policy training (3).

2.3 Design space of existing RL systems

To understand how existing RL systems support the requirements above, we survey the design space of RL systems. Existing designs can be categorised into three types, *function-based*, *actor-based* and *dataflow-based* (see Fig. 2):

(a) **Function-based RL systems** are the most common type. They express RL algorithms typically as Python functions

Type	System	Execution	Distribution	Acceleration	Algorithm
Function-based	SEED RL [9]	Python functions	environment only	DNNs	actor/learner/env
	Acme [17]	Python components	delegated to backend		agent
	RLGraph [43]				
Actor-based	Ray [33]	task (stateless)	local scheduler	DNNs	Python functions with Ray API [33]
	RLlib [24]	actor (stateful)	global scheduler		
	MALib [56]		RPC		
Dataflow-based	Podracer [15]	JIT-compiled by JAX [11]	two hard-coded distribution schemes	funcs/DNNs/envs	JAX [11] API
	RLlib Flow [25]	predefined dataflow operators	sharded dataflow operators with Ray tasks [33]	DNNs	Operator API
	WarpDrive [22]	GPU thread blocks	✗	CUDA kernels	CUDA
Fragmented dataflow graph	MSRL	heterogeneous dataflow fragments	dataflow partitioning	funcs/operators/DNNs/envs	agent/actor/learner/env

Tab. 1: Design space of distributed RL systems

executed directly by workers (see Fig. 2a). The RL training loop is implemented using direct function calls. For example, *Acme* [17] and *SEED RL* [9] organise algorithms as actor/learner functions; *RLGraph* [43] uses a component abstraction, and users register Python callbacks to define functionality. Distributed execution is delegated to backend engines, e.g. TensorFlow [13], PyTorch [38], Ray [33].

(b) **Actor-based** RL systems execute algorithms through message passing between a set of (programming language) actors deployed on worker nodes (see Fig. 2b). *Ray* [33] defines algorithms as parallel tasks in an actor model. Tasks are distributed among nodes using remote calls. Defining control flow in a fully distributed model, however, is burdensome. To overcome this issue, *RLlib* [24] adds logically centralised control on top of Ray. Similarly, *MALib* [56] offers a high-level agent/evaluator/learner abstraction for population-based MARL algorithms (e.g. PSRO [34]) using Ray as a backend.

(c) **Dataflow-based** RL systems define algorithms through data-parallel operators, which are mapped to GPU kernels or distributed tasks (see Fig. 2c). Operators are typically predefined, and users must choose from a fixed set of APIs. For example, *Podracer* [15] uses JAX [11] to compile subroutines as dataflow operators for distributed execution on TPUs. *WarpDrive* [22] defines dataflow operators as CUDA kernels, and executes the complete RL training loop using GPU thread blocks. *RLlib Flow* [25] uses distributed dataflow operators, implemented as iterators with message passing.

Tab. 1 considers how well these approaches satisfy our four requirements from §2.2:

Execution abstraction. Function- and actor-based systems execute RL algorithms directly through implemented (Python) functions and user-defined (programming language) actors, respectively. This prevents systems from applying optimisations how RL algorithms are parallelised or distributed. In contrast, dataflow-based systems execute computation using pre-defined/compiled operators [15, 25] or CUDA kernels [22], which offers optimisation opportunities.

Distribution strategies. Most function-based systems adopt a fixed strategy that distributes actors to parallelise the environment execution (①+② in Fig. 1) with only a single learner. Actor-based systems distribute stateful actors and stateless tasks across multiple workers, often using a greedy scheduler without domain-specific planning.

Dataflow-based systems typically hardcode how dataflow operators are assigned to workers. *Podracer* [15] provides two strategies: *Anakin* co-hosts an environment and an agent on each TPU core; *Sebulba* distributes the environment, learners and actors on different TPU cores; and *RLlib Flow* [25] shards dataflow operators across distributed Ray actors.

Acceleration support. Most RL systems only accelerate DNN policy inference and training (①+③). Some dataflow-based systems (e.g. *Podracer* [15] and *WarpDrive* [22]) also accelerate other parts of training, requiring custom dataflow implementations: e.g. *Podracer* can accelerate the environment execution (②) on TPU cores; *WarpDrive* executes the entire training loop (①–③) on a single GPU using CUDA.

Algorithm abstraction. Function-based RL systems make it easy to provide intuitive actor/learner/env APIs. Actor-based RL systems often provide lower-level harder-to-use APIs for distributed components (e.g. Ray’s *get/wait/remote* [33]); higher-level libraries (e.g. *RLlib*’s *PolicyOptimizer API* [24]) try to bridge this gap. Dataflow-based systems come with fixed dataflow operators, requiring users to rewrite algorithms. For example, JAX [11] provides the *vmap* operator for vectorisation and *pmap* for single-program multiple-data (SPMD) parallelism.

In summary, there is an opportunity to design a new RL system that combines the usability of function-based systems with the acceleration potential of dataflow-based systems. Such a design requires a new execution abstraction that retains the flexibility to apply different acceleration and distribution strategies on top of an RL algorithm specification.

Algorithm 1: MAPPO algorithm in MSRL

```

1 class MAPPOAgent(Agent):
2 def act(self, state):
3 return self.actors.act(state)
4 def learn(self, sample):
5 return self.learner.learn(sample)

6 class MAPPOActor(Actor):
7 def act(state):
8 action = self.actor_net(state)
9 #@MSRL.fragment(type='Action', ops=['AllGather'],
10 data=[action])
11 reward, new_state = MSRL.env_step(action)
12 #@MSRL.fragment(type='Step', ops=['AllGather'], data
13 =[reward, new_state])
14 return reward, new_state

15 class MAPPOLearner(Learner):
16 def learn(sample):
17 action, reward, state, next_state = sample
18 last_pred = self.critic_net(next_state)
19 pred = self.critic_net(state)
20 r = discounted_reward(reward, last_pred, self.gamma)
21 adv = gae(reward, next_state, pred, last_pred, self.
22 gamma)
23 for i in range(self.iter):
24 loss += self.mappo_net_train(action, state, adv, r)
25 return loss / self.iter

26 class MAPPOTrainer(Trainer):
27 def train(self, episode):
28 for i in range(episode):
29 state = MSRL.env_reset()
30 #@MSRL.fragment(type='Reset', ops=['AllGather'],
31 data=[state])
32 for j in range(self.duration):
33 reward, new_state = MSRL.agent_act(state)
34 MSRL.replay_buffer_insert(reward, new_state)
35 sample = MSRL.replay_buffer_sample()
36 #@MSRL.fragment(type='Buffer', ops=['AllGather'],
37 data=[sample])
38 loss = MSRL.agent_learn(sample)
39 #@MSRL.fragment(type='Learner', ops=['AllGather'],
40 data=[actor_net.get_trainable_params()])

41 mappo_algorithm_config = {
42 'agent': {'num': 4, 'type': MAPPOAgent,
43 'actor': MAPPOActor, 'learner': MAPPOLearner
44 },
45 'actor': {'num': 1, 'type': MAPPOActor,
46 'policy': MAPPOActorNet, 'env': True},
47 'learner': {'num': 1, 'type': MAPPOLearner,
48 'policy': [MAPPOCriticNet, MAPPONetTrain],
49 'params': {'gamma': 0.9}},
50 'env': {'type': MPE, 'num': 32, 'params': {'name': 'MPE'}}

51 mappo_deployment_config = {
52 'workers': [198.168.152.19, 198.168.152.20, [...]
53 'GPUs_per_worker': 2,
54 'distribution_policy': 'Single_learner_coarse'}

```

3 MSRL API

Next, we introduce MSRL’s API and give an example of how it can implement the multi-agent PPO (MAPPO) algorithm [53]. The API separates the RL algorithm’s logic from deployment and execution considerations.

A user expresses an RL algorithm through familiar concepts, such as agents, actors, learners, trainers and environments. An *agent* consists of actors and learners: *actors* collect data from the *environment*, and *learners* manage the training policy. A *trainer* provides the training loop logic, specifying the interaction between actors and learners for each agent.

MSRL offers two types of APIs: (i) a *component API* defines the behaviour of each algorithmic component, defined through abstract classes. For example, `Actor.act()`

specifies the interaction between actors and environments; `Learner.learn()` implements the training logic of the neural network; a training loop is defined through `Trainer.train()`; and (ii) an *interaction API* allows components to interact. For example, an actor submits the collected training data using `MSRL.replay_buffer_insert()`; a learner samples from the replay buffer using `MSRL.replay_buffer_sample()`.

MSRL determines how the algorithm is deployed through two configurations: (1) an *algorithm configuration* defines the logical components (i.e. agents, actors, learners etc.) and their hyper-parameters; and (2) a *deployment configuration* refers to a *distribution policy* and the devices.

Example. Alg. 1 sketches the MAPPO implementation. Its policies and DNNs are omitted for simplicity. `MAPPOAgent` (line 1) defines the agent behaviour: it interacts with the environment through `MAPPOActor` (line 6), and performs the policy training with `MAPPOLearner` (line 13). It then collects experiences from the environment with a given policy (lines 8–10), which is used to optimise the DNN model (lines 15–21). To define behaviour, `MAPPOAgent`, `MAPPOActor` and `MAPPOLearner` inherit from base classes, overriding abstract methods with the algorithm’s logic.

`MAPPOTrainer` defines the training loop (line 23) and uses MSRL’s interaction API. After entering the loop (line 25), it resets the environment using `MSRL.env_reset()`. It then uses `MSRL.agent_act()` to collect the experience (line 29) from `MAPPOActor`, and saves it in the replay buffer (line 30). Finally, the trainer calls `MSRL.agent_learn()` to execute the `learn()` function from `MAPPOLearner`.

Partition annotations. Despite defining an RL algorithm in a classical way with actors, learners and trainers, MSRL must be able to decompose the algorithm and distribute computation across devices. Since auto-distributing code is a hard problem [1, 2, 41], MSRL relies on user *annotations* in the code to help identify suitable partitioning boundaries.

The *partition annotations* in lines 9, 11, 27, 32, 34 denote possible boundaries in the algorithm for parallel and distributed execution. Each annotation specifies the type of code fragment and what dependent data must be transferred at the boundary when computation is distributed. Code between two consecutive partition annotations thus becomes a self-contained *fragment*, which can be assigned to a device.

As an example, consider the fragment defined by the annotations in lines 9 and 11: the first annotation stipulates that an action can be received from the previous fragment before interacting with the environment; the second annotation sends the reward and `new_state` to the next fragment on another device. As we explain in the next section, this enables MSRL to distribute the environment simulation across devices.

The **algorithm configuration** (lines 35–43) is a Python dictionary that defines how to instantiate the algorithmic components (lines 35). It specifies their number, type and hyper-parameters, which MSRL requires for execution (see §5). In

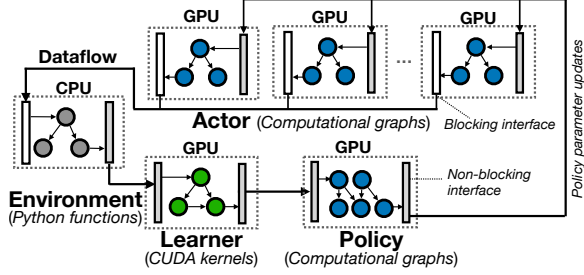


Fig. 3: Translating functions to fragmented dataflow graphs

this example, the training uses 4 agents, each with 1 actor and 1 learner; and each actor interacts with 32 environments.

The **deployment configuration** (lines 44–47) specifies how the computation is executed through a *distribution policy*. With the help of the partition annotations, the distribution policy governs the partitioning of the algorithmic components and their distribution. We discuss partitioning and distribution policies in §4 and §6, respectively.

4 Translation to Fragmented Dataflow Graphs

We now describe how MSRL uses fragmented dataflow graphs to decouple the parallelisation and distribution of RL algorithms from their implementation.

4.1 Fragmented dataflow graphs

MSRL must partition an RL algorithm so that it can be distributed across workers. Since it is challenging to parallelise and distribute the algorithm implementation directly, MSRL introduces a new execution abstraction by representing the algorithm as a *fragmented dataflow graph* (FDG): each node in the FDG is a potentially data-parallel fragment of code, which can be deployed on workers with GPUs and CPUs. FDGs thus allow MSRL to execute the RL computation on different devices depending on the allocation of fragments. MSRL distributes fragments to devices on remote workers, which then exchange data over the network; or fragments may be co-located on a single worker and use shared memory communication.

Fig. 3 gives a high-level overview of an FDG, which consists of multiple dataflow *fragments* (dashed square nodes). A fragment encompasses the dataflow graph of the corresponding code with two interfaces: an *entry* and an *exit* interface. These interfaces implement the functionality for sharing data with other fragments: if fragments are located on the same worker, they can directly share data structures; if they belong to different workers, they can use network communication operators. Depending on the communication method, the interface may be blocking (e.g. when using shared data structures) or non-blocking (e.g. for asynchronous communication).

Each fragment must be allocated to a device. Depending on how a fragment’s code is implemented, fragments require specific hardware resources for execution. For example, the *actor* and the *policy* fragments in Fig. 3 are implemented

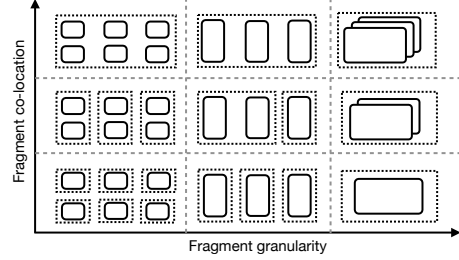


Fig. 4: Fragment granularity vs. fragment co-location

using the data-parallel operators of a DL engine, and thus require a GPU for execution; the *environment* fragment has a native Python implementation that executes on a CPU.

MSRL parallelises the execution of fragment code by creating multiple instances of it and assigning each instance to a separate device. All such replicated fragments share the same interface, allowing MSRL to use the communication operation from the partition annotation to synchronise data (see §3). For example, if the fragment denoted by the partition annotations in lines 32 and 34 in Alg. 1 is replicated, the instances synchronise using the AllGather method.

4.2 Deployment using fragment dataflow graphs

When deploying an RL algorithm as an FDG, two dimensions impact execution performance (see Fig. 4):

(1) **Fragment granularity** refers to a fragment’s code size, which affects device utilisation. A small fragment may under-utilise a GPU; a large one may exhaust GPU memory.

The fragment granularity also determines the ratio between computation and communication. The frequency and amount of data exchanged during synchronisation between fragments is a major source of overhead, often limiting scalability. In general, coarser fragments require less synchronisation, which reduces communication overhead, but they diminish opportunities for parallelism. For example, multiple fragments may exchange policy parameters (e.g. weights) or the replay buffer (i.e. trajectories) frequently at each step; alternatively, they may batch data from multiple steps and communicate at each episode to increase network efficiency.

FDGs can thus subsume the existing execution strategies of current RL systems. Based on the partition annotations, an FDG may fuse an actor and environment into one CPU-based fragment, and a learner into a GPU-based fragment (e.g. as proposed by Acme [17]); alternatively, it can create a coarser-grained GPU fragment by moving the DNN from the CPU fragment to the learner, which accelerates policy inference (as done by SEED RL [9]); at the coarsest granularity, an even larger fragment may contain the actor, learner, DNNs and environment, which accelerates the whole training loop (as done by WarpDrive [22] or Anakin [15]).

(2) **Fragment co-location** refers to the mapping of fragments to devices on the same worker. Co-locating fragments avoids network communication (Ethernet or InfiniBand) for synchronisation. Instead, it uses intra-node communication (NVLink

Algorithm 2 Fragmented dataflow graph generation

```

1: function GENERATE_FDG(algorithm)
2:   FDG ← {}
3:   DFG ← generate_dfg(algorithm)
4:   boundary ← annotation_parser(annotations)
5:   common_node ← label_common_node(DFG, boundary)
6:   for node in common_node do
7:     sub_graph ← graph_traversal(node, DFG)
8:     fragment ← generate_interface(sub_graph, boundary)
9:     FDG ← FDG ∪ fragment
10:  return FDG

```

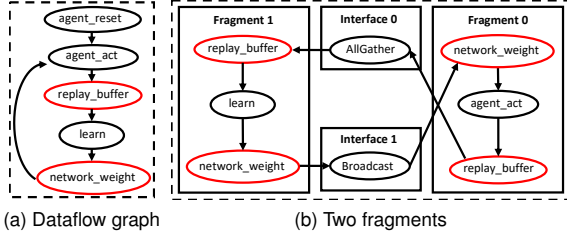


Fig. 5: Example of FDG construction for MAPPO

or PCIe), which reduces latency and increases throughput. Whether co-location is feasible depends on the available resources (e.g. the number of GPUs per node) and fragment constraints (e.g. the resource needs of fragments).

Choosing the right trade-off between fragment granularity and co-location is key to achieving good performance. The FDG abstraction allows MSRL to make different trade-offs using a set of distribution policies. Next, we describe how MSRL transforms an RL algorithm into an FDG.

4.3 Building fragmented dataflow graphs

MSRL generates an FDG by partitioning the algorithm’s dataflow graph. Based on the user-specified partition annotations (§3), it splits the dataflow graph into fragments, which then exchange the data specified by the annotations.

Alg. 2 shows the algorithm to generate an FDG. First, it statically analyses the RL algorithm to construct a dataflow graph, and then it partitions the graph into fragments.

Recall that the partition annotations denote the boundaries between code segments and describe the data that must be transferred when the code is partitioned. Correspondingly, in the partitioned fragments, the nodes that represent the data specified by the partitioned annotation must be at the boundary of fragments. We refer to these nodes as *common* nodes in the dataflow graph. MSRL creates fragments by partitioning the graph at the common nodes.

Consider the partitioning of the MAPPO algorithms from Alg. 1 with the two annotations in lines 32 and 34. Fig. 5a shows its simplified dataflow graph, with the data described by the two annotations highlighted in red. By splitting the graph at the common nodes, it can be partitioned into two fragments (see Fig. 5b). In each fragment, the common nodes (circled in red) are connected to interface implementations, which are generated for a given communication method.

To perform the partitioning, Alg. 2 first parses the partition annotations to record the communication method and corre-

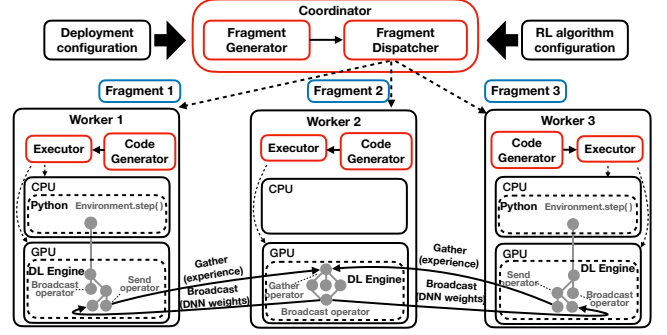


Fig. 6: Overview of the MSRL architecture

sponding data for each fragment boundary (line 4) and uses this information to label the common nodes (line 5). It then traverses the dataflow graph from each common node (line 7). The traversal terminates when it reaches another common node or a leaf node, and the constructed subgraph forms a new fragment. The algorithm also duplicates the common nodes in the original dataflow graph and fragment graph. Since the subgraph between two common nodes can only belong to one fragment, the algorithm removes the subgraph from the original dataflow graph after constructing the fragment, removing it from the following search. Finally, it adds the implementation of the communication interfaces and connects the common nodes with the interfaces (line 8).

If the user does not provide any partition annotations, MSRL, by default, partitions the algorithm along the algorithmic components, i.e. actors, learners, environments etc. Each component’s input and output values are the common nodes in the dataflow graph. The communication method is chosen by analysing the dataflow between the components.

5 MSRL Architecture

We describe MSRL’s architecture, which follows a coordinator/worker design (see Fig. 6): (1) a user submits the RL algorithm implementation to a coordinator; (2) the coordinator generates the FDG and dispatches fragments to workers; and (3) workers generate executable code for the received fragments, which can be run by e.g. a DL engine.

5.1 Generating and dispatching fragments

The coordinator has two components:

The **FDG Generator** uses the FDG generation algorithm (Alg. 2) to partition the RL algorithm based on the partition annotations and to insert code for the interfaces.

To ensure the code is executable by a given DL engine, a user must implement parts of the RL algorithm using appropriate dataflow operators, such as `Mul()`, `Div()` etc. For the generated fragment interfaces, MSRL maintains a mapping from the operations defined by the partition annotations to the corresponding dataflow operators. For example, the `AllGather` annotation in Alg. 1 maps to a `comms.AllGather` operator [19] in the MindSpore DL engine.

The generated code is synthesised as part of the `run()`

Distribution policy	Deployment	Description
<p>[DP-A]: Single learner/coarse</p> <p>replicate: (<i>actor, env</i>) split: (<i>learner</i>)</p> <p>e.g. Acme [17], Sebulba [15]</p>		<p>DP-A replicates the actor and environment fragments: W1–W3 co-locate 1 GPU fragment with an actor for DNN policy inference and 1 CPU fragment for the environment policy execution. A single GPU fragment with a learner performs policy training (W4), gathering batched training data, training the policy and broadcasting updates.</p>
<p>[DP-B] – Single learner/fine</p> <p>replicate: fused <i>actor/env</i> split: <i>learner</i></p> <p>e.g. SEED RL [9]</p>		<p>DP-B fuses the actor and environment into 1 fragment (W1–W3) but handles policy inference at the learner (W4), i.e. actors do not contain DNNs. W4 executes policy inference and training in 1 GPU fragment; W1–3 only have CPU fragments. W4 scatters actions to W1–W3 and gathers data for policy training.</p>
<p>[DP-C] – Multiple learners</p> <p>replicate: fused <i>actor/learner, env</i></p>		<p>DP-C performs data-parallel training with multiple learners, supporting fully decentralised MARL training [6, 39, 55, 57]. DP-C co-locates 2 fragments: a GPU fragment that fuses the actor and learner, accelerating policy inference, training and replay buffer management, and a CPU fragment for environment execution.</p>
<p>[DP-D] – GPU only</p> <p>replicate: fused <i>actor/learner/env</i></p>		<p>DP-D fuses the training loop into 1 GPU fragment. To enable communication among GPU fragments, DP-D uses Allreduce operators compiled into the computational graph with NCCL2 [36]. DP-D is a distributed implementation of the single-node systems (e.g. WarpDrive [22]).</p>
<p>[DP-E] – Environments</p> <p>replicate: fused <i>actor/learner</i> split: <i>env</i></p> <p>e.g. MALib [56]</p>		<p>DP-E has a dedicated worker for environment execution. W1 has CPU fragments to execute environment instances on multiple CPU cores; W2–W4 fuse the actor and learner to accelerate policy inference and training. W1 gathers the inferred actions and scatters the states and rewards.</p>
<p>[DP-F] – Central</p> <p>replicate: fused <i>actor/learner, env</i> split: <i>param server/policy pool</i></p>		<p>DP-F supports a central <i>policy pool</i> [56] or <i>parameter server</i> [23] on a separate worker (W1). W2–W4 co-locate GPU fragments for policy inference and training and CPU fragments for environment execution.</p>

Tab. 2: Default distribution policies supported by MSRL

method of a Fragment template class. A worker then executes the fragment by invoking this method.

The **Fragment Dispatcher** launches multiple instances of the DL engine on each worker, and sets up the distributed infrastructure for communication, e.g. through MPI [29]. It also assigns fragments to devices according to the specified distribution policy and sends the fragments to the workers.

5.2 Executing fragments on workers

Each worker also has two components:

The **Code Generator** produces executable code that is spe-

cific to a given execution environment, such as DL engine, for the fragments received from the coordinator. Based on the fragment’s AST, it also synthesises the interface implementations. Finally, it converts the AST to Python code using the `unparse()` function from the Python AST library.

When a worker is assigned multiple fragment replicas on a single GPU, it uses several CUDA streams concurrently, one for each fragment. This approach, however, incurs an overhead launching and scheduling streams and also leads to extra memory copies between the CPU and GPU. MSRL avoids this by *fusing* co-located fragments into a single one.

This leverages the support of DL engines to process data in a SIMD fashion: by batching tensors from multiple replicated fragments into a single tensor, they can be processed by the DL engine’s data-parallel operators.

To fuse fragments, the Code Generator locates the AST node for the tensor in the fragment. Since the Python AST represents a tensor’s shape and data as a list stored in the `elts` field, the Code Generator can create the appropriate tensor shape for a batched operator.

The **Executor** launches the generated fragment code on different devices based on their implementations. For example, code implemented using MindSpore operators can run on a GPU controlled by the MindSpore DL engine; pure Python fragments execute on CPU cores. For efficient GPU execution, DL engines such as MindSpore compile code into a computational graph with GPU kernels. This enables optimisations: e.g. independent operators can be scheduled in parallel, improving performance over sequential execution.

Communication between fragments is also handled by MindSpore operators, which automatically select a suitable implementation based on the device type and network topology. It may use NCCL [36] for multi-GPU collective communication and MPI [29] for InfiniBand traffic between workers.

6 Distribution Policies

A distribution policy governs how MSRL executes an RL algorithm by specifying the FDG partitioning and the mapping of fragments to workers and devices. In general, there is not a single policy that is optimal in all cases: the performance and applicability of a policy depends on the type of RL algorithm, the size and complexity of the DNN model, its hyper-parameters, the available cluster compute resources (i.e. CPUs and GPUs), and the network bandwidth. MSRL allows users to switch easily between policies, either for the same RL algorithm or when using different algorithms.

Tab. 2 describes MSRL’s six default policies, showing the trade-off between them. These policies largely follow the hard-coded distribution strategies of existing RL systems; further policies can be defined easily by expert users:

DP-A (Single learner/coarse) replicates the actor and environment fragments but relies on a single learner. The DNN policy is replicated across the actors and learner, which only requires coarse synchronisation. This policy is therefore suitable for expensive environments that need scaling out, but small DNN models that can be synchronised in a batched fashion.

In contrast, *DP-B (Single learner/fine)* fuses the actor and environment into a single CPU fragment, and only deploys the learner on a GPU. Therefore it does not communicate policy parameters between workers, which is preferable for large DNN models with many parameters. Compared to the DP-A, it relies on fine-grained synchronisation: training data is exchanged at each step, instead of being batched per episode. For good performance, DP-B therefore requires high bandwidth

connectivity between workers.

DP-C (Multiple learners) performs data-parallel training with multiple learners. This policy is necessary when the data generated from actors becomes too large for a single GPU, and e.g. DP-A cannot be used. However, it requires the tuning of hyper-parameters (e.g. the learning rate) to scale due to its reliance on data parallelism. Since workers only exchange information about the trained policy (e.g. aggregated DNN gradients), DP-C is communication efficient.

DP-D (GPU only) fuses the full RL training loop into a single GPU fragment. It is only applicable if the environment has a GPU implementation. Since the full RL training loop is accelerated, DP-D achieves the highest performance by eliminating the overhead of CPU/GPU switches.

DP-E (Environments) dedicated one or more workers for the execution of environments. It is best suited when the RL training job executes computationally expensive CPU environments, e.g. complex physics simulations, which requires many dedicated CPU cores for execution.

Finally, *DP-F (Central)* introduces a separate fragment for a centralised policy pool [56] or parameter server [23]. It can support CTDE-based MARL algorithms (similar to Ray [33] and RLlib [24]) by workers sending local policy updates to a parameter server; or population-based MARL (similar to MALib [56]) by a worker maintaining a population of policies, selecting the optimal one and broadcasting it to other workers.

7 Evaluation

Our experimental evaluation answers the following questions: “what are the trade-offs between distribution policies?” (§7.2); “what is MSRL’s performance compared to other systems?” (§7.3); and “how well does MSRL scale?” (§7.4).

7.1 Experimental set-up

Implementation and test-bed. We implement MSRL on top of MindSpore [18]. The code is available at <https://github.com/mindspore-ai/reinforcement>. We conduct the experiments on both a *cloud* and a *local* cluster. As shown in Tab. 3, the cloud cluster has 16 VMs; the local cluster has 4 nodes. All machines run Ubuntu Linux 20.04 with CUDA 11.03, cuDNN 8.2.1, OpenMPI 4.0.3 and MindSpore 1.8.0.

RL algorithms and environments. We answer the above questions by focusing on three widely-used RL algorithms, Proximal Policy Optimization (PPO) [45], its multi-agent version, Multi-Agent PPO (MAPPO) [53], and Asynchronous Advantage Actor Critic (A3C) [30]. The policy uses a seven-layer DNN. As environments, we use three games from MuJoCo [49], an advanced physics simulation engine, and the Multi-Agent Particle Environment (MPE) [27], a set of mixed cooperative-competitive environments for MARL.

Distribution policies. With the above algorithms, we use the following distribution policies from Tab. 2: DP-A (Single

Cluster	CPU cores #nodes × #per node	GPUs #nodes × #per node	Interconnects intra-, inter-node
Azure VMs NC24s_v2	Intel Xeon E5-2690 16×24, 448 GB	P100, 16×4	PCIe, 10 GbE
Local cluster	Intel Xeon 8160 4×96, 250 GB	V100, 4×8	NVLink, 100 Gbps IB

Tab. 3: Testbed configuration

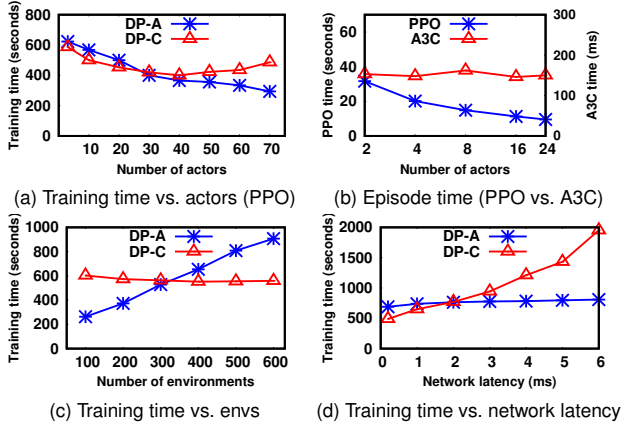


Fig. 7: Impact of hyper-parameters and network properties

learner/coarse), DP-B (Single learner/fine), DP-C (Multiple learners), DP-D (GPU only) and DP-E (Environments).

Metrics. For PPO, we measure (i) the training time to reach a given reward value and (ii) the time for each episode. For MAPPO, as the problem size increases with the number of agents due to agent competition, we report training time against the problem complexity and the training throughput.

7.2 Trade-offs between distribution policies

First we observe the impact of changes to the RL workload and hardware resources on different distribution policies.

Actors. We investigate the impact of the number of actors used when training PPO to a reward of 3,000 with 200 environments. We report the trade-off between two policies, DP-A (Single learner/coarse) and DP-C (Multiple learners).

Fig. 7a shows the training time with 2 to 70 actors. DP-A scales better than DP-C with more actors: it converges faster with a higher actor count. DP-C achieves the best performance with 40 actors, and its performance deteriorates after that but it outperforms DP-A with fewer than 30 actors.

Since DP-A only has 1 learner, its training batch size is fixed. Increasing the number of actors therefore only distributes environment execution. In contrast, DP-C fuses actors and learners into single fragments. With more actors, it also adds learners and thus reduces the batch size for each learner. This adds randomness to the training [16] and affects converge speed. In general, DP-C needs further hyper-parameter tuning (e.g. of the learning rate) for better performance [16].

Next we compare the behaviour of two algorithms, PPO and A3C, under the same distribution policy DP-A. Fig. 7b shows the time per episode for up to 24 actors. (Note that A3C requires at least 2 actors.) Under DP-A, PPO’s episode

time decreases as the number of actors increases; in contrast, A3C’s episode time stays constant with the actor count.

In PPO, adding actors increases the parallelism degree of environment execution and therefore reduces the workload per actor; in A3C, each actor only interacts with one environment, making its workload independent of the actor count. To reduce the time per episode for A3C, a new distribution policy could be written that distributes the actor among multiple devices, e.g. exploiting data- or task-parallelism.

Environments. We investigate the impact of changing the number of environments. When an agent interacts with more environments in parallel within one episode, it trains with more data, thus potentially improving training performance. We fix the number of actors to 50.

Fig. 7c shows the training time as we vary the number of environments from 100 to 600 under DP-A and DP-C. DP-C scales better than DP-A with more environments, and there is a cross-over point with 320 environments. The training time with DP-A increases with more environments but remains stable for DP-C. This is because DP-A’s actors send trajectories to the learner, which increases in communication overhead with more environments. In contrast, DP-C only communicates gradients and its communication overhead is fixed. Therefore the right distribution policy must be selected based on the environment count.

Network latency. We also examine the behaviour of DP-A and DP-C when deployed with PPO on clusters with different network latencies. We change the network latency in our cloud cluster using the Linux traffic control (tc) tool from 0.2 ms to 6 ms. We use 400 environments and 50 actors.

Fig. 7d reports training time. DP-C is more sensitive to network latency than DP-A. Its training time increases rapidly with higher network latency, while remaining stable for DP-A. Since DP-C leverages Mindspore’s data parallel model [18] to broadcast, aggregate and update gradients, it repeatedly transmits many small tensors; DP-A transmits the trajectory and DNN model weights as compact large tensors, performing data transmissions less frequently. However, DP-C transmits less data than DP-A and thus is more appropriate in clusters with low network latencies (below 2 ms).

Cluster size. Finally, we compare the performance of PPO under 3 distribution policies when increasing the number of GPUs (Fig. 8): DP-A and DP-B use a single learner but apply different synchronisation granularities; DP-C scales to multiple learners using data-parallelism. We use a fixed number of 320 Mujoco HalfCheetah [5] environments.

Fig. 8a shows the training time to reach a reward of 4,000 in the cloud cluster with up to 64 GPUs; Fig. 8b reports the time per episode. Compared to 1 GPU, all distribution policies reduce training time with more GPUs. With 64 GPUs, DP-A achieves the highest speed-up in training time ($5.3\times$). Compared to that, DP-B exhibits a longer training time, which is lowest for 16 GPUs. DP-A maintains local copies of the

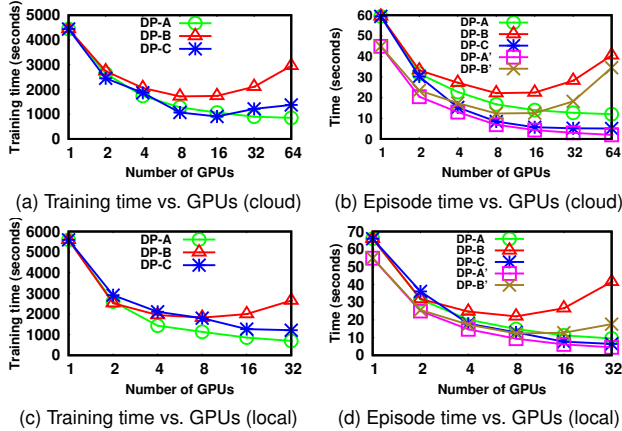


Fig. 8: Impact of GPU number on training time

DNN model at the actor and learner, and only actors send the batched states and rewards to the learner at the end of each episode (i.e. after 1,000 steps). This reduces the overhead with a large number of GPUs compared to DP-B, whose actor fragments must communicate with the learner at each step.

DP-C exhibits a different behaviour: with 16 GPUs, it achieves better performance than either DP-A and DP-B. This is because it distributes policy training: it trains smaller batches of trajectories on each device and aggregates the gradients from all devices to update the policy. Instead, DP-B and DP-A gather all batches and train them using 1 learner.

While DP-C is the best policy choice for 16 GPUs, it performs worse than DP-A for a larger cluster. With more GPUs, trajectory batches become smaller and aggregating the trained gradients becomes less efficient compared to training a single large batch. Therefore, although DP-C trains each episode faster than DP-A (see Fig. 8b), it requires more episodes to reach a similar reward value.

Note that DP-A and DP-B use the original implementation of the PPO algorithm [45], which uses a single learner to train the policy. As a result, scalability is constrained by the centralised policy training (⊙ in Fig. 1). To ignore this bottleneck in the algorithm, we also exclude the policy training time in Fig. 8b, labelled DP-A' and DP-B'. Here, MSRL continues scaling even with large GPU numbers: when moving from 32 to 64 GPUs, performance increases by 25%.

In Figs. 8c and 8d, we repeat the same experiment on the local cluster, which has faster GPU and network connectivity (NVLink, InfiniBand). When comparing Figs. 8c and 8a, we can see that DP-A now always performs better than DP-C, irrespective of the GPU count. Since the local cluster supports faster GPU communication, DP-A's overhead is lower than in the cloud cluster. DP-A's larger batches become more effective than DP-C's training/aggregation over smaller batches.

Conclusions: As the GPU count, hyper-parameters or network properties change, the differences between the synchronisation granularity and frequency of distribution policies impact performance. MSRL's ability to select a distribution policy at deployment time allows users to achieve the best perfor-

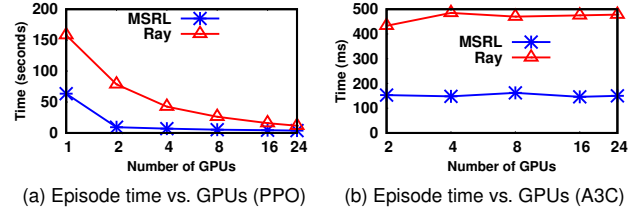


Fig. 9: Performance comparison with Ray

mance in different configurations without having to change the algorithm implementation.

7.3 Performance against baseline systems

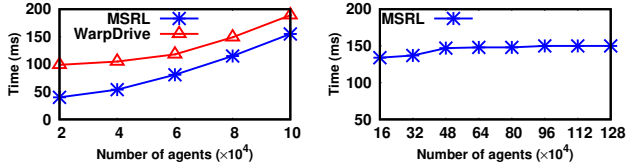
We want to put the absolute performance of MSRL into perspective by comparing against other RL systems that hard-code particular parallelisation and distribution strategies. For the comparison, we choose Ray [33], as a representative distributed RL training system, and WarpDrive [22], as a single-GPU system that parallels the complete RL training loop.

Distributed training. We compare against Ray [33] using PPO and A3C with DP-A on the local cluster. Both algorithms are implemented and tuned based on Ray's public PyTorch-based implementation [40]. We measure the time per episode, which is dominated by actor and environment execution. Since the time spent on DNN training/inference is negligible, the fact that MSRL and Ray use different DL frameworks (MindSpore vs. PyTorch) has low impact.

Fig. 9a shows PPO's time per episode. In this experiment, we distribute 320 environments evenly among the actors, i.e. each actor interacts with $320/\#actors$ environments, and a single learner trains the DNN. As shown in the figure, MSRL's episode time with 1 GPU is $2.5\times$ faster than Ray's because Ray executes the actor on the CPU, which then interacts with all environments sequentially. As the number of GPUs increases, both systems reduce episode time as each actor interacts with fewer environments. With 24 GPUs, it takes 3.85 s for MSRL to execute an episode compared to 11.38 s for Ray ($3\times$ speed-up). When actors interact with multiple environments, MSRL combines DNN inference into one operation through FDG fusion, exploiting GPU parallelism better. It also uses fragments to execute environment steps in parallel by launching multiple processes.

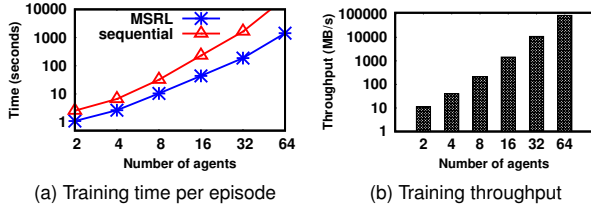
Fig. 9b shows A3C's time per episode. Here, 1 learner performs gradient optimisation with gradients collected asynchronously from actors. Each actor interacts with 1 environment and computes gradients locally. The figure shows that both systems' time per episode remains constant with more GPUs. Each GPU is mapped to one actor, and its workload remains unchanged. Again, MSRL executes actors $2.2\times$ faster than Ray: since its distribution policy exploits asynchronous send/receive operations from NCCL, MSRL avoids further data copies between GPU and CPU. In contrast, Ray copies data to the CPU to communicate asynchronously.

GPU only training. Next, we deploy PPO with distribution policy DP-D, which fuses the training loop into a single GPU



(a) Episode time vs. agents (1 GPU) (b) Episode time vs. agents (GPUs)

Fig. 10: Scalability of GPU-only PPO



(a) Training time per episode

(b) Training throughput

Fig. 11: Scalability with agent count (MAPPO)

fragment and replicates it for distributed execution. We use PPO with the MPE *simple tag* environment [27], which simulates a predator-prey game in which chaser agents are rewarded for catching runner agents. Runner agents are penalised for being caught by a chaser or colliding with runners.

After adapting the *simple tag* implementation to GPUs, we train different numbers of agents (thus increasing the number of environments) on the local cluster and measure the training time per episode. We compare against WarpDrive [22], which performs single-GPU end-to-end RL training.

Fig. 10a shows the training time on 1 GPU. Compared to WarpDrive, MSRL is $1.2\times$ – $2.5\times$ faster when ranging from 20,000 to 100,000 agents. MSRL’s DL engine (MindSpore) compiles fragments to computational graphs, exploiting more parallelisation and optimisation opportunities.

Fig. 10b shows how MSRL scales to multiple GPUs (which is unsupported by WarpDrive) when each GPU trains 80,000 agents. The training time increases from 138 ms to 150 ms from 160,000 to 960,000 agents. Beyond that, it remains stable – the available connectivity bandwidth (NVLink, InfiniBand) now bounds the communication overheads between GPU fragments and devices.

Conclusions: MSRL’s FDG abstraction provides the flexibility to use distribution policies for PPO and A3C that are tailored to their bottlenecks, e.g. enabling parallel environment execution and aggressively parallelising GPU execution. Ray is limited by the distribution strategy of its RLlib library; WarpDrive’s manual CUDA implementation prevents it from leveraging more sophisticated compiler optimisations.

7.4 Scalability

We explore how MSRL’s design scales as we increase the number of deployed agents for a MARL algorithm and the number of environments (thus increasing the amount of training data). We want to validate if MSRL’s approach introduces scalability bottlenecks.

Agents. We increase the number of agents for the MAPPO MARL algorithm with the MPE *simple spread* [27] environ-

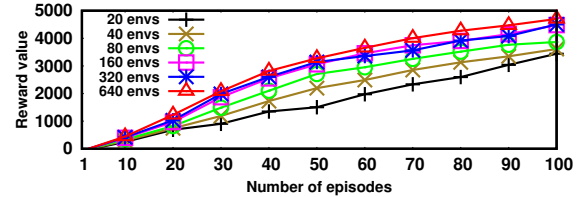


Fig. 12: Statistical efficiency with environment count (PPO)

ment, where n agents interact and learn to cover n landmarks (rewards) while avoiding collisions (penalties). In addition to training local observations, agents must also train global observations on how far the closest agent is to each landmark. This results in $O(n^3)$ observations with n agents, thus quickly growing the computation complexity and GPU memory footprint [27]. We deploy the MAPPO agents on the cloud cluster using DP-E: each GPU on a worker trains 1 agent, and a dedicated worker executes all environments.

Fig. 11a shows the training time per episode for up to 64 GPUs against a sequential baseline (1 GPU). Due to its cubic complexity, the training time increases sharply both for the baseline and MSRL. With distributed training, MSRL’s training time grows more slowly than the baseline: when training 32 agents, MSRL improves the performance by $58\times$; with 64 agents, the baseline exhausts GPU memory, while MSRL trains one episode in 23.8 mins.

Fig. 11b compares the throughput when training different numbers of agents. The throughput is measured as the amount of data trained per second (in MB/s). Increasing the agent number (i.e. GPU devices) significantly improves throughput, and the margin becomes larger with more GPUs: the throughput when training 64 agents is over $7,600\times$ higher than training 2 agents. This is because multiple GPUs train agents in parallel, and more agents result in more training data (i.e. a larger size of observations) per GPU.

Environments. Next we increase the number of environments and observe the impact on the statistical efficiency, i.e. the number of episodes to reach a given reward value. We assign 10 environments to each CPU and add more devices in the cloud cluster using DP-A. We expect MSRL to achieve higher statistical efficiency with more training data.

In Fig. 12, we show the reward along with the number of episodes for different environment counts. As expected, increasing the number of environments leads to a higher reward value. As more CPUs execute environments, more trajectories are used per episode, achieving a higher reward.

Conclusions: MSRL’s FDG abstraction does not deteriorate scalability. MSRL scales with a large number of data-intensive agents, handling the increase in communication between fragments without bottlenecks. As expected, a larger amount of data generated by more environments also increases the statistical efficiency of the training process.

8 Conclusions

We described *MindSpore Reinforcement Learning* (MSRL), a system that supports the flexible parallelisation and distribution of RL algorithms on multiple devices. MSRL separates the algorithm implementation from its execution through the abstraction of fragmented dataflow graphs (FDGs), which enable MSRL to support diverse distribution policies for allocating code fragments to devices. Our experimental results show the trade-offs when using different distribution policies.

References

- [1] Michael Bauer, Wonchan Lee, Elliott Slaughter, Zhihao Jia, Mario Di Renzo, Manolis Papadakis, Galen Shipman, Patrick McCormick, Michael Garland, and Alex Aiken. Scaling implicit parallelism via dynamic control replication. In *Proceedings of the 26th ACM SIGPLAN Symposium on Principles and Practice of Parallel Programming*, PPOPP '21, page 105–118, New York, NY, USA, 2021. Association for Computing Machinery.
- [2] Michael Bauer, Sean Treichler, Elliott Slaughter, and Alex Aiken. Legion: Expressing locality and independence with logical regions. In *Proceedings of the 2012 International Conference for High Performance Computing, Networking, Storage and Analysis*, SC '12, page 1–11, USA, 2012. IEEE Computer Society.
- [3] Christopher Berner, Greg Brockman, Brooke Chan, Vicki Cheung, Przemyslaw Debiak, Christy Dennison, David Farhi, Quirin Fischer, Shariq Hashme, Christopher Hesse, Rafal Józefowicz, Scott Gray, Catherine Olsson, Jakub Pachocki, Michael Petrov, Henrique Pondé de Oliveira Pinto, Jonathan Raiman, Tim Salimans, Jeremy Schlatter, Jonas Schneider, Szymon Sidor, Ilya Sutskever, Jie Tang, Filip Wolski, and Susan Zhang. Dota 2 with large scale deep reinforcement learning. *CoRR*, abs/1912.06680, 2019.
- [4] Alexander Brauckmann, Andrés Goens, Sebastian Ertel, and Jerónimo Castrillón. Compiler-based graph representations for deep learning models of code. In Louis-Noël Pouchet and Alexandra Jimborean, editors, *CC '20: 29th International Conference on Compiler Construction, San Diego, CA, USA, February 22-23, 2020*, pages 201–211. ACM, 2020.
- [5] Greg Brockman, Vicki Cheung, Ludwig Pettersson, Jonas Schneider, John Schulman, Jie Tang, and Wojciech Zaremba. Openai gym, 2016.
- [6] Michael Chang, Sidhant Kaushik, S. Matthew Weinberg, Tom Griffiths, and Sergey Levine. Decentralized reinforcement learning: Global decision-making via local economic transactions. In *Proceedings of the 37th International Conference on Machine Learning, ICML 2020, 13-18 July 2020, Virtual Event*, volume 119 of *Proceedings of Machine Learning Research*, pages 1437–1447. PMLR, 2020.
- [7] Tianqi Chen, Thierry Moreau, Ziheng Jiang, Lianmin Zheng, Eddie Q. Yan, Haichen Shen, Meghan Cowan, Leyuan Wang, Yuwei Hu, Luis Ceze, Carlos Guestrin, and Arvind Krishnamurthy. TVM: an automated end-to-end optimizing compiler for deep learning. In Andrea C. Arpaci-Dusseau and Geoff Voelker, editors, *13th USENIX Symposium on Operating Systems Design and Implementation, OSDI 2018, Carlsbad, CA, USA, October 8-10, 2018*, pages 578–594. USENIX Association, 2018.
- [8] Michael Dennis, Natasha Jaques, Eugene Vinitzky, Alexandre M. Bayen, Stuart Russell, Andrew Critch, and Sergey Levine. Emergent complexity and zero-shot transfer via unsupervised environment design. In Hugo Larochelle, Marc’Aurelio Ranzato, Raia Hadsell, Maria-Florina Balcan, and Hsuan-Tien Lin, editors, *Advances in Neural Information Processing Systems 33: Annual Conference on Neural Information Processing Systems 2020, NeurIPS 2020, December 6-12, 2020, virtual*, 2020.
- [9] Lasse Espeholt, Raphaël Marinier, Piotr Stanczyk, Ke Wang, and Marcin Michalski. SEED RL: scalable and efficient deep-rl with accelerated central inference. In *8th International Conference on Learning Representations, ICLR 2020, Addis Ababa, Ethiopia, April 26-30, 2020*. OpenReview.net, 2020.
- [10] Lasse Espeholt, Hubert Soyer, Rémi Munos, Karen Simonyan, Volodymyr Mnih, Tom Ward, Yotam Doron, Vlad Firoiu, Tim Harley, Iain Dunning, Shane Legg, and Koray Kavukcuoglu. IMPALA: scalable distributed deep-rl with importance weighted actor-learner architectures. In Jennifer G. Dy and Andreas Krause, editors, *Proceedings of the 35th International Conference on Machine Learning, ICML 2018, Stockholmsmässan, Stockholm, Sweden, July 10-15, 2018*, volume 80 of *Proceedings of Machine Learning Research*, pages 1406–1415. PMLR, 2018.
- [11] Roy Frostig, Matthew Johnson, and Chris Leary. Compiling machine learning programs via high-level tracing. In *Systems for Machine Learning*, 2018.
- [12] Sven Gronauer and Klaus Diepold. Multi-agent deep reinforcement learning: a survey. *Artificial Intelligence Review*, pages 1–49, 2021.
- [13] Sergio Guadarrama, Anoop Korattikara, Oscar Ramirez, Pablo Castro, Ethan Holly, Sam Fishman, Ke Wang, Ekaterina Gonina, Neal Wu, Efi Kokiopoulou, Luciano Sbaiz, Jamie Smith, Gábor Bartók, Jesse Berent, Chris

- Harris, Vincent Vanhoucke, and Eugene Brevdo. TF-Agents: A library for reinforcement learning in tensorflow. <https://github.com/tensorflow/agents>, 2018. [Online; accessed 25-June-2019].
- [14] Abhishek Gupta, Justin Yu, Tony Z. Zhao, Vikash Kumar, Aaron Rovinsky, Kelvin Xu, Thomas Devlin, and Sergey Levine. Reset-free reinforcement learning via multi-task learning: Learning dexterous manipulation behaviors without human intervention. In *IEEE International Conference on Robotics and Automation, ICRA 2021, Xi'an, China, May 30 - June 5, 2021*, pages 6664–6671. IEEE, 2021.
- [15] Matteo Hessel, Manuel Kroiss, Aidan Clark, Iurii Kemaev, John Quan, Thomas Keck, Fabio Viola, and Hado van Hasselt. Podracer architectures for scalable reinforcement learning. *CoRR*, abs/2104.06272, 2021.
- [16] Elad Hoffer, Itay Hubara, and Daniel Soudry. Train longer, generalize better: closing the generalization gap in large batch training of neural networks. In Isabelle Guyon, Ulrike von Luxburg, Samy Bengio, Hanna M. Wallach, Rob Fergus, S. V. N. Vishwanathan, and Roman Garnett, editors, *Advances in Neural Information Processing Systems 30: Annual Conference on Neural Information Processing Systems 2017, December 4-9, 2017, Long Beach, CA, USA*, pages 1731–1741, 2017.
- [17] Matt Hoffman, Bobak Shahriari, John Aslanides, Gabriel Barth-Maron, Feryal Behbahani, Tamara Norman, Abbas Abdolmaleki, Albin Cassirer, Fan Yang, Kate Baumli, Sarah Henderson, Alexander Novikov, Sergio Gómez Colmenarejo, Serkan Cabi, Çağlar Gülçehre, Tom Le Paine, Andrew Cowie, Ziyu Wang, Bilal Piot, and Nando de Freitas. Acme: A research framework for distributed reinforcement learning. *CoRR*, abs/2006.00979, 2020.
- [18] Huawei. Mindspore. <https://www.mindspore.cn/en>, 2020.
- [19] Huawei. Mindspore all gather operator. https://www.mindspore.cn/docs/en/r1.7/api_python/ops/mindspore.ops.AllGather.html?highlight=allgather, 2022. Accessed: 2022-5-18.
- [20] John Jumper, Richard Evans, Alexander Pritzel, Tim Green, Michael Figurnov, Olaf Ronneberger, Kathryn Tunyasuvunakool, Russ Bates, Augustin Židek, Anna Potapenko, Alex Bridgland, Clemens Meyer, Simon A A Kohl, Andrew J Ballard, Andrew Cowie, Bernardino Romera-Paredes, Stanislav Nikolov, Rishub Jain, Jonas Adler, Trevor Back, Stig Petersen, David Reiman, Ellen Clancy, Michal Zielinski, Martin Steinegger, Michalina Pacholska, Tamas Berghammer, Sebastian Bodenstern, David Silver, Oriol Vinyals, Andrew W Senior, Koray Kavukcuoglu, Pushmeet Kohli, and Demis Hassabis. Highly accurate protein structure prediction with AlphaFold. *Nature*, 596(7873):583–589, 2021.
- [21] Vijay R. Konda and John N. Tsitsiklis. Actor-critic algorithms. In Sara A. Solla, Todd K. Leen, and Klaus-Robert Müller, editors, *Advances in Neural Information Processing Systems 12, [NIPS Conference, Denver, Colorado, USA, November 29 - December 4, 1999]*, pages 1008–1014. The MIT Press, 1999.
- [22] Tian Lan, Sunil Srinivasa, and Stephan Zheng. Warpdrive: Extremely fast end-to-end deep multi-agent reinforcement learning on a GPU. *CoRR*, abs/2108.13976, 2021.
- [23] Mu Li, David G. Andersen, Jun Woo Park, Alexander J. Smola, Amr Ahmed, Vanja Josifovski, James Long, Eugene J. Shekita, and Bor-Yiing Su. Scaling distributed machine learning with the parameter server. In Jason Flinn and Hank Levy, editors, *11th USENIX Symposium on Operating Systems Design and Implementation, OSDI '14, Broomfield, CO, USA, October 6-8, 2014*, pages 583–598. USENIX Association, 2014.
- [24] Eric Liang, Richard Liaw, Robert Nishihara, Philipp Moritz, Roy Fox, Ken Goldberg, Joseph Gonzalez, Michael I. Jordan, and Ion Stoica. Rllib: Abstractions for distributed reinforcement learning. In Jennifer G. Dy and Andreas Krause, editors, *Proceedings of the 35th International Conference on Machine Learning, ICML 2018, Stockholmsmässan, Stockholm, Sweden, July 10-15, 2018*, volume 80 of *Proceedings of Machine Learning Research*, pages 3059–3068. PMLR, 2018.
- [25] Eric Liang, Zhanghao Wu, Michael Luo, Sven Mika, and Ion Stoica. Distributed reinforcement learning is a dataflow problem. *CoRR*, abs/2011.12719, 2020.
- [26] Timothy P. Lillicrap, Jonathan J. Hunt, Alexander Pritzel, Nicolas Heess, Tom Erez, Yuval Tassa, David Silver, and Daan Wierstra. Continuous control with deep reinforcement learning. In Yoshua Bengio and Yann LeCun, editors, *4th International Conference on Learning Representations, ICLR 2016, San Juan, Puerto Rico, May 2-4, 2016, Conference Track Proceedings*, 2016.
- [27] Ryan Lowe, Yi Wu, Aviv Tamar, Jean Harb, Pieter Abbeel, and Igor Mordatch. Multi-agent actor-critic for mixed cooperative-competitive environments. In Isabelle Guyon, Ulrike von Luxburg, Samy Bengio, Hanna M. Wallach, Rob Fergus, S. V. N. Vishwanathan, and Roman Garnett, editors, *Advances in Neural Information Processing Systems 30: Annual Conference on Neural Information Processing Systems 2017, December 4-9, 2017, Long Beach, CA, USA*, pages 6379–6390, 2017.

- [28] Luo Mai, Guo Li, Marcel Wagenländer, Konstantinos Fertakis, Andrei-Octavian Brabete, and Peter R. Pietzuch. Kungfu: Making training in distributed machine learning adaptive. In *14th USENIX Symposium on Operating Systems Design and Implementation, OSDI 2020, Virtual Event, November 4-6, 2020*, pages 937–954. USENIX Association, 2020.
- [29] Message Passing Interface Forum. *MPI: A Message-Passing Interface Standard Version 4.0*, June 2021.
- [30] Volodymyr Mnih, Adrià Puigdomènech Badia, Mehdi Mirza, Alex Graves, Tim Harley, Timothy P. Lillicrap, David Silver, and Koray Kavukcuoglu. Asynchronous methods for deep reinforcement learning. In *Proceedings of the 33rd International Conference on International Conference on Machine Learning - Volume 48, ICML’16*, page 1928–1937. JMLR.org, 2016.
- [31] Volodymyr Mnih, Adrià Puigdomènech Badia, Mehdi Mirza, Alex Graves, Timothy P. Lillicrap, Tim Harley, David Silver, and Koray Kavukcuoglu. Asynchronous methods for deep reinforcement learning. In Maria-Florina Balcan and Kilian Q. Weinberger, editors, *Proceedings of the 33rd International Conference on Machine Learning, ICML 2016, New York City, NY, USA, June 19-24, 2016*, volume 48 of *JMLR Workshop and Conference Proceedings*, pages 1928–1937. JMLR.org, 2016.
- [32] Volodymyr Mnih, Koray Kavukcuoglu, David Silver, Andrei A. Rusu, Joel Veness, Marc G. Bellemare, Alex Graves, Martin A. Riedmiller, Andreas Fiedjeland, Georg Ostrovski, Stig Petersen, Charles Beattie, Amir Sadik, Ioannis Antonoglou, Helen King, Dharshan Kumaran, Daan Wierstra, Shane Legg, and Demis Hassabis. Human-level control through deep reinforcement learning. *Nat.*, 518(7540):529–533, 2015.
- [33] Philipp Moritz, Robert Nishihara, Stephanie Wang, Alexey Tumanov, Richard Liaw, Eric Liang, Melih Elilbol, Zongheng Yang, William Paul, Michael I. Jordan, and Ion Stoica. Ray: A distributed framework for emerging AI applications. In Andrea C. Arpaci-Dusseau and Geoff Voelker, editors, *13th USENIX Symposium on Operating Systems Design and Implementation, OSDI 2018, Carlsbad, CA, USA, October 8-10, 2018*, pages 561–577. USENIX Association, 2018.
- [34] Paul Muller, Shayegan Omidshafiei, Mark Rowland, Karl Tuyls, Julien Pérolat, Siqi Liu, Daniel Hennes, Luke Marris, Marc Lanctot, Edward Hughes, Zhe Wang, Guy Lever, Nicolas Heess, Thore Graepel, and Rémi Munos. A generalized training approach for multiagent learning. In *8th International Conference on Learning Representations, ICLR 2020, Addis Ababa, Ethiopia, April 26-30, 2020*. OpenReview.net, 2020.
- [35] Ranjit Nair, Milind Tambe, Makoto Yokoo, David V. Pynadath, and Stacy Marsella. Taming decentralized pomdps: Towards efficient policy computation for multiagent settings. In Georg Gottlob and Toby Walsh, editors, *IJCAI-03, Proceedings of the Eighteenth International Joint Conference on Artificial Intelligence, Acapulco, Mexico, August 9-15, 2003*, pages 705–711. Morgan Kaufmann, 2003.
- [36] NVIDIA. NCCL: Nvidia collective communications library, 2022. [Online; accessed 10-December-2021].
- [37] Johan Samir Obando-Ceron and Pablo Samuel Castro. Revisiting rainbow: Promoting more insightful and inclusive deep reinforcement learning research. In Marina Meila and Tong Zhang, editors, *Proceedings of the 38th International Conference on Machine Learning, ICML 2021, 18-24 July 2021, Virtual Event*, volume 139 of *Proceedings of Machine Learning Research*, pages 1373–1383. PMLR, 2021.
- [38] Adam Paszke, Sam Gross, Francisco Massa, Adam Lerer, James Bradbury, Gregory Chanan, Trevor Killeen, Zeming Lin, Natalia Gimelshein, Luca Antiga, Alban Desmaison, Andreas Köpf, Edward Z. Yang, Zachary DeVito, Martin Raison, Alykhan Tejani, Sasank Chilamkurthy, Benoit Steiner, Lu Fang, Junjie Bai, and Soumith Chintala. Pytorch: An imperative style, high-performance deep learning library. In Hanna M. Wallach, Hugo Larochelle, Alina Beygelzimer, Florence d’Alché-Buc, Emily B. Fox, and Roman Garnett, editors, *Advances in Neural Information Processing Systems 32: Annual Conference on Neural Information Processing Systems 2019, NeurIPS 2019, December 8-14, 2019, Vancouver, BC, Canada*, pages 8024–8035, 2019.
- [39] Chao Qu, Shie Mannor, Huan Xu, Yuan Qi, Le Song, and Junwu Xiong. Value propagation for decentralized networked deep multi-agent reinforcement learning. In Hanna M. Wallach, Hugo Larochelle, Alina Beygelzimer, Florence d’Alché-Buc, Emily B. Fox, and Roman Garnett, editors, *Advances in Neural Information Processing Systems 32: Annual Conference on Neural Information Processing Systems 2019, NeurIPS 2019, December 8-14, 2019, Vancouver, BC, Canada*, pages 1182–1191, 2019.
- [40] Ray. Ray ppo setting, last checked: 10/09/2022. https://github.com/ray-project/ray/blob/master/rllib/tuned_examples/ppo/halfcheetah-ppo.yaml, 2020.
- [41] Christopher J. Rossbach, Yuan Yu, Jon Currey, Jean-Philippe Martin, and Dennis Fetterly. Dandelion: A compiler and runtime for heterogeneous systems. In *Proceedings of the Twenty-Fourth ACM Symposium on*

- Operating Systems Principles*, SOSP '13, page 49–68, New York, NY, USA, 2013. Association for Computing Machinery.
- [42] Nadav Rotem, Jordan Fix, Saleem Abdulrasool, Summer Deng, Roman Dzhubarov, James Hegeman, Roman Levenstein, Bert Maher, Nadathur Satish, Jakob Olesen, Jongsoo Park, Artem Rakhov, and Misha Smelyanskiy. Glow: Graph lowering compiler techniques for neural networks. *CoRR*, abs/1805.00907, 2018.
- [43] Michael Schaarschmidt, Sven Mika, Kai Fricke, and Eiko Yoneki. Rlgraph: Modular computation graphs for deep reinforcement learning. In Ameet Talwalkar, Virginia Smith, and Matei Zaharia, editors, *Proceedings of Machine Learning and Systems 2019, MLSys 2019, Stanford, CA, USA, March 31 - April 2, 2019*. mlsys.org, 2019.
- [44] Julian Schrittwieser, Ioannis Antonoglou, Thomas Hubert, Karen Simonyan, Laurent Sifre, Simon Schmitt, Arthur Guez, Edward Lockhart, Demis Hassabis, Thore Graepel, et al. Mastering atari, go, chess and shogi by planning with a learned model. *Nature*, 588(7839):604–609, 2020.
- [45] John Schulman, Filip Wolski, Prafulla Dhariwal, Alec Radford, and Oleg Klimov. Proximal policy optimization algorithms. *CoRR*, abs/1707.06347, 2017.
- [46] David Silver, Aja Huang, Chris J. Maddison, Arthur Guez, Laurent Sifre, George van den Driessche, Julian Schrittwieser, Ioannis Antonoglou, Vedavyas Panneershelvam, Marc Lanctot, Sander Dieleman, Dominik Grewe, John Nham, Nal Kalchbrenner, Ilya Sutskever, Timothy P. Lillicrap, Madeleine Leach, Koray Kavukcuoglu, Thore Graepel, and Demis Hassabis. Mastering the game of go with deep neural networks and tree search. *Nat.*, 529(7587):484–489, 2016.
- [47] Peng Sun, Jiechao Xiong, Lei Han, Xinghai Sun, Shuxing Li, Jiawei Xu, Meng Fang, and Zhengyou Zhang. Tleague: A framework for competitive self-play based distributed multi-agent reinforcement learning. *CoRR*, abs/2011.12895, 2020.
- [48] Richard S Sutton and Andrew G Barto. *Reinforcement learning: An introduction*. MIT press, 2018.
- [49] Emanuel Todorov, Tom Erez, and Yuval Tassa. Mujoco: A physics engine for model-based control. In *2012 IEEE/RSJ International Conference on Intelligent Robots and Systems*, pages 5026–5033. IEEE, 2012.
- [50] Oriol Vinyals, Igor Babuschkin, Wojciech M. Czarnecki, Michaël Mathieu, Andrew Dudzik, Junyoung Chung, David H. Choi, Richard Powell, Timo Ewalds, Petko Georgiev, Junhyuk Oh, Dan Horgan, Manuel Kroiss, Ivo Danihelka, Aja Huang, Laurent Sifre, Trevor Cai, John P. Agapiou, Max Jaderberg, Alexander Sasha Vezhnevets, Rémi Leblond, Tobias Pohlen, Valentin Dalibard, David Budden, Yury Sulsky, James Molloy, Tom Le Paine, Çağlar Gülçehre, Ziyu Wang, Tobias Pfaff, Yuhuai Wu, Roman Ring, Dani Yogatama, Dario Wunsch, Katrina McKinney, Oliver Smith, Tom Schaul, Timothy P. Lillicrap, Koray Kavukcuoglu, Demis Hassabis, Chris Apps, and David Silver. Grandmaster level in starcraft II using multi-agent reinforcement learning. *Nat.*, 575(7782):350–354, 2019.
- [51] Ronald J. Williams. Simple statistical gradient-following algorithms for connectionist reinforcement learning. *Mach. Learn.*, 8:229–256, 1992.
- [52] XLA and TensorFlow teams. XLA: Optimizing compiler for machine learning, 2022. [Online; accessed 10-December-2021].
- [53] Chao Yu, Akash Velu, Eugene Vinitzky, Yu Wang, Alexandre Bayen, and Yi Wu. The surprising effectiveness of ppo in cooperative multi-agent games, 2021.
- [54] Matei Zaharia, Reynold S. Xin, Patrick Wendell, Tathagata Das, Michael Armbrust, Ankur Dave, Xiangrui Meng, Josh Rosen, Shivaram Venkataraman, Michael J. Franklin, Ali Ghodsi, Joseph Gonzalez, Scott Shenker, and Ion Stoica. Apache spark: a unified engine for big data processing. *Commun. ACM*, 59(11):56–65, 2016.
- [55] Kaiqing Zhang, Zhuoran Yang, Han Liu, Tong Zhang, and Tamer Basar. Fully decentralized multi-agent reinforcement learning with networked agents. In Jennifer G. Dy and Andreas Krause, editors, *Proceedings of the 35th International Conference on Machine Learning, ICML 2018, Stockholm, Sweden, July 10-15, 2018*, volume 80 of *Proceedings of Machine Learning Research*, pages 5867–5876. PMLR, 2018.
- [56] Ming Zhou, Ziyu Wan, Hanjing Wang, Muning Wen, Runzhe Wu, Ying Wen, Yaodong Yang, Weinan Zhang, and Jun Wang. Malib: A parallel framework for population-based multi-agent reinforcement learning. *CoRR*, abs/2106.07551, 2021.
- [57] Matthieu Zimmer, Claire Glanois, Umer Siddique, and Paul Weng. Learning fair policies in decentralized cooperative multi-agent reinforcement learning. In Marina Meila and Tong Zhang, editors, *Proceedings of the 38th International Conference on Machine Learning, ICML 2021, 18-24 July 2021, Virtual Event*, volume 139 of *Proceedings of Machine Learning Research*, pages 12967–12978. PMLR, 2021.